Random Response and Noise Transmission of Discretely Stiffened Composite Panels

Constantinos S. Lyrintzis*
San Diego State University, San Diego, California
and
Rimas Vaicaitis†
Columbia University, New York, New York

The surface protection systems of aerospace and aircraft structures are lately more often constructed from discretely stiffened composite panels. Composite materials proved to be suitable for those structural applications. This paper presents an analytical study on dynamic response and structure-borne sound transmission of these structures due to random loading conditions. A generalized transfer matrix procedure for composite-stiffened flat panels is developed to obtain the required dynamic response solution. Modal decomposition is used to predict the interior noise transmission. The acoustic enclosure is taken to be rectangular in shape. A portion of the boundaries is elastic (composite material), whereas the remaining surface is acoustically rigid. Numerical results are presented for acousto-structural applications.

Nomenclature

a,b,d = cavity dimensions in y,x,z directions, in.
$B(\omega)$ = bulk reactance
c = viscous damping coefficient for the plate, lb-s/in.^{3}
c_0 = speed of sound in the cavity, in./s
D_{11},D_{12},D_{16} D_{26},D_{22},D_{66} = anisotropic plate rigidities, lb − in.
E = Young's modulus, psi
E_{11},E_{22} = orthotropic elastic modulii in a composite ply parallel and perpendicular to the fibers, respectively, psi
F_0 = random point force, lb
f = frequency, Hz
f_u = upper cutoff frequency, Hz
g_{11},g_{22},g_{12} = loss factors, %
G = isotropic shear modulus, psi
G_{12} = shear modulus for composite plies, psi
h = plate thickness, in.
i = $\sqrt{-1}$
L_x = width of the panel (see Fig 1.), in.
M_{0x},M_{0y} = random point couples acting on a plane parallel to x and y, respectively, lb − in.
n = intex number of panel normal modes in x-direction.
p = acoustic pressure, psi
p_0 = reference pressure, psi
p^r,p^e = external and cavity pressure, psi
$\bar{Q}_{ij}$ = reduced stiffnesses relating stress to strain in a composite ply, psi
R = flow resistivity, lb − s/in.^{4} (or mks rayls/m)
$\dot{s}$ = flow rate, in./s
S_p = cross spectral density of random pressure, psi^2/Hz
SPL = sound pressure levels, dB
$S^s(x,\omega)$ = deflection response spectral density at location s, in.^{2}/Hz
S_{F_i} = spectral density of random point forces, lb^2/Hz
$S_{M_{0i}}$ = spectral density of random point couples, lb^2 − in.^{2}/Hz
t = time, s
w = normal displacement of the flexible panel, in.
x,y,z = spatial coordinates, in.
x_s,y_s = coordinates of an arbitrary point at location s on the panel (see Fig. 1), in.
y_m = length of the mth panel, in.
z_k = z-direction distance from panel middle surface to bottom of the kth layer, in.
$Z_A(\omega)$ = absorbent wall impedance
α = angle of fiber direction to a specified boundary axis of the panel, *deg*
β = acoustic dumping coefficient, lb − s/in.^{3}
δ = Dirac delta function
Δf = frequency bandwidth, Hz
$\Delta\omega$ = circular frequency bandwidth, rad/s
ν = isotropic plate Poisson's ratio
ν_{12} = composite ply Poisson's ratio
ξ_{ij} = acoustic modal damping, %
ρ = panel mass density, lb − s^2/in.^{4}
ϱ = air density, lb − s^2/in.^{4}
ω = frequency, rad/s
ω_{ij0} = acoustic modal frequencies, rad/s
ω_0 = lowest acoustic modal frequency, rad/s

Subscripts and Superscripts

n = integer designating the nth mode in x direction
k = integer designating the kth layer of a composite panel
j = refers to jth station
r,l = r = right, l = left, referring to a station

Received Sept. 13, 1988; revision received Aug. 23, 1989.

*Assistant Professor, Department of Aerospace Engineering and Engineering Mechanics. Member AIAA.
†Professor, Department of Civil Engineering and Engineering Mechanics. Member AIAA.

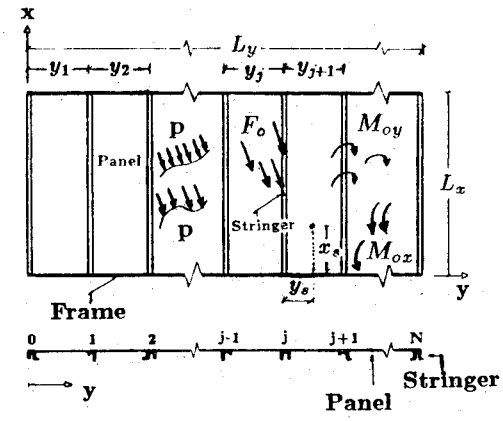

Fig. 1 Stiffened multispanned panel array.

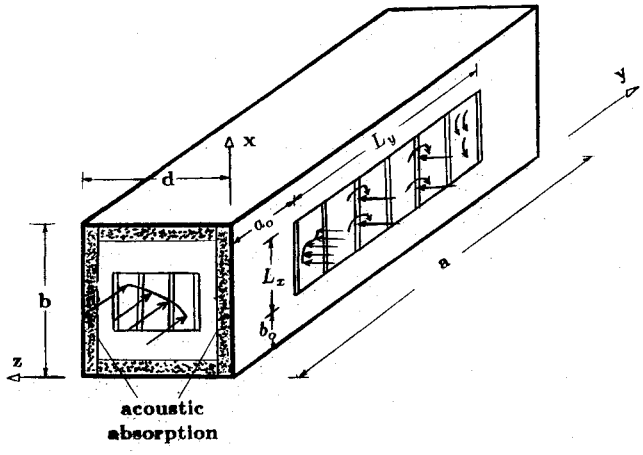

Fig. 2 Geometry of an acoustic enclosure and a stiffened structure.

Introduction

AEROSPACE and aircraft structures are built from many discretely stiffened components. The vibrations induced from power plants, life support systems, thrusters, mechanical and electrical equipment, etc. could generate structure-borne noise in the interior of aircraft and space transportation vehicles. To accommodate the necessary utilities and service functions of those structures, new design concepts for lower weight, extended service life and reduced cost are needed.[1,2] The new generation of composite materials can offer high strength-to-weight and stiffness-to-weight ratios, savings in manufacturing time and cost, and ease of repair.[3,4] The proposed design of the Space Station will involve activities associated with developing a wide technology base in the areas of scientific and commercial endeavors.[1,2] Noise and vibrations will have a direct effect on the quality and limitations of the high precision requirements of many scientific experiments and manufacturing processes that are being proposed for Space Station applications. A similar technology base is needed for the advanced propeller-powered aircraft[5,6] VSTOL, the STOL aircraft, and the tilt-rotor aircraft.[4] This presents a challenge to develop a new technology for noise and vibration control. In general, transmission of structure-borne noise is not well understood, and the information that is presently available is very limited. Hence, fundamental theoretical and experimental work is needed.[7-10]

An analytical study of structure-borne noise generation and transmission into cylindrical shells due to mechanical point loads has been presented in Refs. 9 and 10. Procedures for response and noise transmission estimates were developed for aluminum and fiber-reinforced composite materials. However, the analytical models developed in these studies do not account for the discrete stiffening effect of the finite structures. Procedures have been developed in Refs. 11 and 12 to study response and noise transmission of stiffened and interconnected structures constructed from homogeneous and isotropic materials. It was shown that dynamic response and transmitted sound are sensitive to the choice of geometric, material and structural parameters, damping and acoustic absorption characteristics, and types of random loading inputs. This paper presents an analytical study to predict dynamic response and noise transmission of discretely stiffened, multilayered composite panels. A typical geometry of a stiffened panel is shown in Fig. 1 and of a rectangular enclosure in Fig. 2. The stringer-panel systems have been studied extensively by the transfer matrix approach.[12-16] A detailed analysis based on transfer matrices has been developed to model isotropic-stiffened panels.[12,13,15] The present approach extends those procedures to fiber-reinforced composite materials and more generalized random loading conditions.[17-19] The sound pressure levels in the interior of the enclosure are obtained by coupling the acoustic field to the sidewall vibrations of the stiffened structure.[20] Modal decomposition of the interior acoustic pressure is used together with the point impedance representation[21,22] of the interior acoustic absorption characteristics to solve the governing equations of motion.

Response of a Composite Stiffened Panel to Random Loads

The noise transmitted into the enclosure shown in Fig. 2 is a function of the sidewall response $w(x,y,t)$. Thus, the response characteristics of a multilayered, composite stiffened panel have to be determined first. A detailed response analysis for isotropic materials has been presented in Refs. 12, 13, and 15. In what follows, a brief description on the calculation of vibration response of a stiffened composite sidewall is given.

Consider a flat stiffened panel located on the sidewall at $z = 0$, $b_0 \le x \le b_0 + L_x$, $a_0 \le y \le a_0 + L_y$ is simply supported at the edges normal to the stiffeners as shown in Fig. 1. Using classical thin-plate theory, the equation of motion governing the bending vibrations of a symmetrically layered composite panel located between any two arbitrary stiffeners is[17,12]

$$D_{11}w_{,xxxx} + 4D_{16}w_{,xxxy} + 2(D_{12} + 2D_{66})w_{,xxyy}$$

$$+ 4D_{26}w_{,xyyy} + D_{22}w_{,yyyy} + c\dot{w} + \rho h\ddot{w}$$

$$= p^r(x,y,t) + p^e(x,y,0,t) + F_0(t)\delta(x - x_0)\delta(y - y_0)$$

$$+ M_{0y}(t)\delta(x - x_0)\delta'(y - y_0) + M_{0x}(t)\delta'(x - x_0)\delta(y - y_0) \tag{1}$$

where a comma denotes the partial differential with respect to the subscript, $w(x,y,t)$ is the normal deflection, c is the viscous damping coefficient, ρ is the panel mass density, and h is the plate thickness. The D_{ij} terms are the anisotropic plate rigidity values that relate the internal bending and twisting moments of the plate to the curvatures and twists they induce. Also, p^r is the external random pressure, and $p^e(x,y,0,t)$ is the acoustic radiation pressure at $z = 0$. When the cavity is sufficiently deep (depth comparable to the other dimensions) and the plate is sufficiently stiff (small transverse displacements), the cavity pressure loading on the panel response can be neglected.[20,23,24] In Eq. (1), δ is the Dirac delta function and a prime denotes a derivative, $F_0(t)$ is the random point load, and

$M_{0x}(t)$, $M_{0y}(t)$ are the random point couples acting on a plane parallel to x and y, respectively.

If the plate is hybrid (differing materials across the thickness) composite, then the total mass density can be calculated from[18]

$$\rho = \frac{1}{h}\sum_{k=1}^{N}\rho_k(z_k - z_{k-1}) \tag{2}$$

where z_k is the z-direction distance from the middle surface to the bottom of the kth layer (see Fig. 3). For the case of many layered-symmetric, angle-ply laminates, D_{16} and D_{26} are quite small when compared to the other rigidity values D_{ij} so that orthotropic analysis may be used.[8,17] The following anlysis is based on the previous assumption. The flexural rigidities are given as[17,18]

$$D_{ij} = \frac{1}{3}\sum_{k=1}^{n}(\bar{Q}_{ij})_k(z_k^3 - z_{k-1}^3); \qquad i,j = 1,2,6 \tag{3}$$

where $(\bar{Q}_{ij})_k$ are the reduced stiffnesses for the kth layer, which relate the stresses to the strains in that layer.

The solution for the panel deflection w can be written as

$$w(x,y,t) = \sum_{n=1}^{\infty} q_n(y,t)X_n(x) \tag{4}$$

where X_n are the normal modes corresponding to the x direction, and q_n are the generalized coordinates. Since the panel is simply supported at the edges normal to the stiffeners, the normal modes are $X_n(x) = \sin(n\pi x/L_x)$. Using the above mentioned assumptions (i.e., $D_{16} = D_{26} = p^e = 0$) taking Fourier transformation of Eqs. (1) and (4) and following the Galerkin procedure, Eq. (1) reduces to

$$\frac{d^4\bar{q}_n}{dy^4} - 2\left(\frac{n\pi}{L_x}\right)^2\frac{D_3}{D_{22}}\frac{d^2\bar{q}_n}{dy^2} + \beta_n^4\bar{q}_n = Q_n \tag{5}$$

where

$$\beta_n^4 = \left(\frac{n\pi}{L_x}\right)^4\frac{D_{11}}{D_{22}} + \frac{ic\omega}{D_{22}} - \frac{\rho h\omega^2}{D_{22}} \tag{6}$$

$$D_3 = D_{12} + 2D_{66} \tag{7}$$

$$i = \sqrt{-1} \tag{8}$$

$$Q_n(y,\omega) = \frac{2}{D_{22}L_x}\left[\int_0^{L_x}\bar{p}^r(x,y,\omega)X_n(x)\,dx + \bar{F}_0(\omega)X_n(x_0)\delta(y - y_0) + \bar{M}_{0y}(\omega)X_n(x_0)\delta'(y - y_0) + \bar{M}_{0x}(\omega)X_n'(x_0)\delta(y - y_0)\right] \tag{9}$$

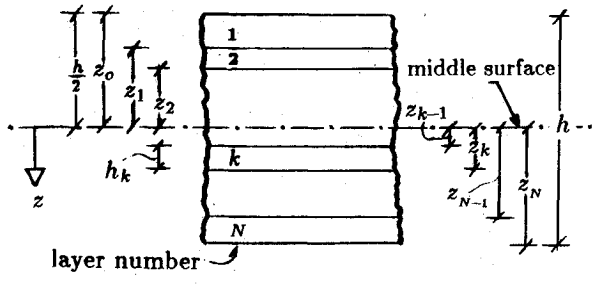

Fig. 3 Geometry of an n-layered laminate.

The roots of the characteristic equation corresponding to assumed solutions of the homogeneous form of Eq. (5) are $\pm\sigma_{1n}$, $\pm i\sigma_{2n}$, where

$$\sigma_{1,2n} = \left\{\left[\frac{1}{D_{22}}\left(\frac{n\pi}{L_x}\right)^4\left(\frac{D_3^2}{D_{22}} - D_{11}\right) + \frac{\rho h\omega^2}{D_{22}} - \frac{ic\omega}{D_{22}}\right]^{1/2} \pm \left(\frac{n\pi}{L_x}\right)^2\frac{D_3}{D_{22}}\right\}^{1/2} \tag{10}$$

The solution to Eq. (5) can be written as a superposition of homogeneous and particular solutions[12,13]

$$\bar{q}_n(y,\omega) = \sum_{i=0}^{3}C_{in}f_{in}(y) + \int_0^y f_{3n}(y - \xi)Q_n(\xi,\omega)\,d\xi \tag{11}$$

where C_{in} are arbitrary constants to be determined from the boundary conditions, and functions $f_{in}(y)$ are given in the Appendix.[12,14] Differentiating Eq. (11) and introducing the relationships between various derivatives of $\bar{q}_n(y,\omega)$ in terms of slope, bending moment and shear, the response of a composite panel can be written in a convenient state vector form[19]

$$\{Z_n\} = \{\delta_n,\theta_n,M_n,V_n\}^T \tag{12}$$

where δ_n, θ_n, M_n and V_n are modal components of deflection, slope, moment and shear, respectively, and superscript T denotes transpose. Then, the response state vector at station j on the panel is

$$\{Z_n\}_j^l = [F]_j\{Z_n\}_{j-1}^r + \int_0^{y_j}[F(y_j - \xi)]\{K_n(\xi)\}\,d\xi \tag{13}$$

where the superscripts l and r indicate either the left or right side of station j, respectively, and $\{K_n(\xi)\}$ is the matrix of generalized random forces

$$\{K_n(\xi)\} = \{0,0,0,D_{22}Q_n(\xi,\omega)\}^T \tag{14}$$

Also, $[F]$ is the field transfer matrix which transfers the state vector across the composite panel

$$[F]_j = [B]_j[R]_j[B]_j^{-1} \tag{15}$$

with matrix $[R]$ having the same form as that given in Refs. 12 and 14 (also given in the Appendix), but now Eq. (10) has to be implemented. The new form for matrices $[B]$ and $[B]^{-1}$ is given in the Appendix.

To transfer a state vector across the stiffeners, point transfer matrices need to be developed. The stiffener does not interfere with the continuity of the deflections and slopes in the skin on either side of the line of the attachment.[14] Thus,

$$\{q_n\}_j^r = \{q_n\}_j^l \tag{16}$$

$$\{q_{n,y}\}_j^r = \{q_{n,y}\}_j^l \tag{17}$$

The stiffener produces a change in the moment and shear components of the state vector. The form of change of the state vector has been discussed extensively in Refs. 11, 12, and 15. The procedure is based on the basic deflection equations for the stiffener, that the panel system undergoes negligible lateral motion, and that the slope $w_{,y}$ is equal to the angle of torsional rotation of the stiffener. Thus any kind of stiffeners L, I, T and channel sections (see Fig. 1) can be included by

changing the geometric characteristics of the stiffener. In addition to bending and twisting, axial and thermal loads may also be induced. Modified point transfer matrices have been developed to account for these effects.[11,12,15] Following the procedures presented in Refs. 12 and 14, the transfer across a stiffening element at station j is

$$\{Z_n\}_j^r = [G]_j\{Z_n\}_j^l \tag{18}$$

where $[G]$ is the point transfer matrix. We note that for cases in which the stiffener's material is orthotropic and the fiber orientation does not coincide with the stringer's natural axis (along the length) but forms an angle α, the following transformation should be used to determine the stiffener's modulus of elasticity E_x[18]

$$\frac{1}{E_x} = \frac{\cos^4\alpha}{E_{11}} + \left(\frac{1}{G_{12}} - \frac{2\nu_{12}}{E_{11}}\right)\cos^2\alpha\,\sin^2\alpha + \frac{\sin^4\alpha}{E_{22}} \tag{19}$$

Now the state vector for a multibay panel shown in Fig. 1 can be expressed at any arbitrary location s, where

$$s = y_s + \sum_{m=1}^{j} y_m$$

as

$$\{Z_n\}_s^l = {}_s^l[T]_0^l\{Z_n\}_0^l + {}_s^l\{E_n\}_0^l \tag{20}$$

where matrix ${}_s^l[T]_0^l$ transfers the state vector from station 0 to station s such that

$${}_s^l[T]_0^l = [F_s][G]_j[F]_j[G]_{j-1}\ldots[F]_1[G]_0 \tag{21}$$

in which $[F_s]$ is a field transfer matrix which transfers the state vector over a portion of a panel located between stations j and $j+1$. Transfer matrix ${}_s^l\{E_n\}_0^l$ represents the effect of distributed and concentrated loads

$${}_s^l\{E_n\}_0^l = {}_s^l[T]_1^l\{L_{1n}\} + {}_s^l[T]_2^l\{L_{2n}\} + \ldots + {}_s^l[T]_j^l\{L_{jn}\} + \{L_{sn}\} \tag{22}$$

where

$$\{L_{jn}\} = \int_0^{y_j}[F(y_j-\xi)]\{K_n(\xi)\}\,d\xi \tag{23}$$

and $\{L_{sn}\}$ can be obtained from Eq. (23) by replacing y_j with y_s.

The solution for the state vector $\{Z_n\}_0^l$ in Eq. (20) can be obtained by applying boundary conditions at $y=0$ and $y=L_y$. In this approach, boundaries corresponding to simple (i.e., $\delta_n = M_n = 0$), fixed (i.e., $\delta_n = \theta_n = 0$), free (i.e., $M_n = V_n = 0$), or elastic supports can be considered (not necessarily the same at both ends). Then, after the solution for the state vector $\{Z_n\}_0^l$ is known, the response state vector $\{Z_n\}_s^l$ can be obtained from Eq. (20).[13] Finally, the response state vector in terms of displacement, slope moment, and shear can be obtained at any arbitrary location on the stiffened panel from

$$\{W(x,\omega)\}_s^l = \sum_{n=1}^{\infty}\{Z_n\}_s^l X_n(x) \tag{24}$$

The first element of the response state vector $\{W(x,\omega)\}_s^l$ from Eq. (24) is the displacement component $\bar{w}_s(x,\omega)$, which will be used to obtain a solution for the acoustic pressure inside the enclosure.

Utilizing the theory of random processes, the response spectral densities corresponding to the four elements in the state vector can be obtained from Eq. (24). For example, the deflection response spectral density at location s can be calculated from

$$S^s(x,\omega) = \sum_{n=1}^{\infty}\sum_{m=1}^{\infty} S^s_{\delta_n\delta_m}(\omega)X_n(x)X_m(x) \tag{25}$$

where $S^s_{\delta_n\delta_m}(\omega)$ is the cross-spectral density of the amplitude δ_n^s determined from Eq. (20)

Sound Transmission into Enclosures

Consider a rectangular acoustic space occupying a volume $V = abd$ as shown in Fig. 2. The interior surface of the enclosure is assumed to be covered with absorptive materials for which the impedance characteristics are specified. Noise is generated in the acoustic enclosure through the vibration of the flexible portions of the sidewall, the partitions or the sound sources located in the interior. The perturbation pressure p within the enclosure satisfies the linearized acoustic wave equation[11,20]

$$\nabla^2 p(\underline{x},t) + \beta\dot{p}(\underline{x},t) - \frac{\ddot{p}(\underline{x},t)}{c_0^2} + \varrho\dot{s}\delta(\underline{x}-\underline{x}_0) = 0 \tag{26}$$

where a dot denotes derivative with respect to time, ∇^2 is the Laplacian operator

$$\nabla^2 = \frac{\partial^2}{\partial x^2} + \frac{\partial^2}{\partial y^2} + \frac{\partial^2}{\partial z^2}$$

δ is the Dirac delta function, which locates the point source, $\underline{x}_0 = x_0, y_0, z_0$, $\underline{x} = x, y, z$ and β, c_0, ϱ, $\dot{s}(t)$ are the acoustic damping coefficient, speed of sound, fluid density, and flow rate, respectively.

The boundary conditions to be satisfied by Eq. (26) depend on the interior surface conditions. These conditions could range from acoustically hard walls to those of highly absorbent surfaces which are treated with acoustic insulation materials. At acoustically rigid boundaries

$$\frac{\partial p}{\partial n} = 0 \tag{27}$$

where n is the outward normal to the boundary. Equation (27) is employed when calculating the undamped modes and acoustic modal frequencies in the enclosure. For a vibrating elastic surface at the boundary, the condition to be satisfied is

$$\frac{\partial p}{\partial n} = -\varrho\ddot{w} \tag{28}$$

where w is the normal displacement of the wall. For interior surfaces treated with absorbent materials, the point impendance[21] and/or the bulk reaction[22] models can be used to model these boundary conditions:

$$\frac{\partial p}{\partial n} = -\frac{\varrho\dot{p}}{Z_A(\omega)} \tag{29}$$

$$\frac{\partial p}{\partial n} = -\frac{\varrho[\dot{p} + B(\omega)\nabla_s^2\dot{p}]}{Z_A(\omega)} \tag{30}$$

where Z_A, B, ∇_s^2 are respectively the absorbent wall impedance, the bulk reactance, and the Laplacian at the interior

surface boundary. The point reaction model given in Eq. (29) assumes only local fluid-solid interaction, whereas the bulk reactance model characterized by Eq. (30) includes on the average, the effect of the entire acoustic surface. For the absorbent and vibrating surface, Eqs. (28), (29), and (30) can be combined to prescribe the required boundary conditions.

The solution for acoustic pressure p has been presented in Refs. 11 and 20. Then, the sound pressure levels inside the enclosure can be calculated from

$$SPL(x,y,z,\omega) = 10 \log\left\{S_{\bar{p}}(x,y,z,\omega)\frac{\Delta\omega}{p_0^2}\right\} \tag{31}$$

where $S_{\bar{p}}$ is the spectral density of the interior acoustic pressure, $\Delta\omega$ is the frequency bandwidth, and p_0 is reference pressure ($p_0 = 2.9 \times 10^{-9}$ psi, $p_0 = 20\mu N/m^2$).

Noise generated in the interior by other vibrating surfaces such as partitions or other sidewalls can be calculated in a similar fashion by the procedure presented in Refs. 11 and 12. Then, the total acoustic pressure generated by different vibrating sources can be obtained from[11]

$$p = p_1 + p_2 + \ldots p_m \tag{32}$$

where $p_1, p_2, \ldots, p_m$ are the acoustic pressure contributions from the vibrating walls which surround the enclosure. If those pressure contributions are assumed to be independent, the cross-spectral densities corresponding to the various pressure components can be set equal to zero thereby simplifying the calculation procedure.

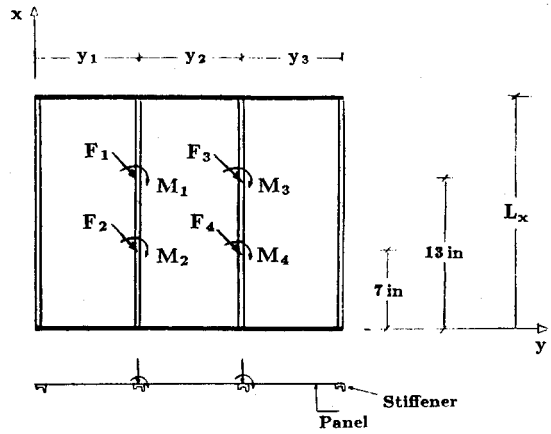

Fig. 4 A three-bay stiffened panel.

Numerical Results

Numerical results have been obtained for simplified versions of the stiffened structure shown in Figs. 1 and 2. The stiffened panel is composed of three equal bays. Two stiffeners are located at the boundaries, and others are placed at a distance $y_1 = y_2 = y_3 = 8.2$ in. (see Fig. 4). The materials considered for the composite panel are graphite and kevlar. The ply properties are as follows:

$E_{11_g} = 1.987 \times 10^7$ psi $\quad E_{11_k} = 1.102 \times 10^7$ psi

$E_{22_g} = 1.450 \times 10^6$ psi $\quad E_{22_k} = 8.702 \times 10^5$ psi

$G_{12_g} = 7.252 \times 10^5$ psi $\quad G_{12_k} = 2.901 \times 10^5$ psi

$\nu_{12_g} = 0.30$ $\quad \nu_{12_k} = 0.31$

$h_{k_g} = 0.005$ in. $\quad h_{k_k} = 0.005$ in.

$\rho_{k_g} = 1.450 \times 10^{-4}$ lb.s^2/in.^{4} $\quad \rho_{k_k} = 1.273 \times 10^{-4}$ lb.s^2/in.^{4}

where the subscripts g and k indicate graphite and kevlar material, respectively. The physical constants for the stiffeners are cross-sectional area, $A = 0.2302$ in.^{2}, warping constant, $C_{ws} = 0.01649$ in.^{6}, torsion constant, $C = 2.263 \times 10^{-4}$ in.^{4}, second moments of area with respect to the center of gravity, $I_\eta = 0.122$ in.^{4}, $I_{\eta\xi} = 0$, $I_\xi = 0.0183$ in.^{4}. The composite material properties for the stiffeners are the same as for the panel with angle of fiber orientation $\alpha = 0$. Damping in the skin-stringer structure is introduced by replacing E_{11}, E_{22}, G_{12} by $E_{11}(1 + ig_{11})$, $E_{22}(1 + ig_{22})$, $G_{12}(1 + ig_{12})$, respectively, where g_{11}, g_{22}, g_{12} are the loss factors. The loss factor was taken the same for aluminum for comparison reasons. Numerical results were obtained for $g_{11} = g_{22} = g_{12} = 0.02$. The forcing function has the simple form of point forces F_i or point couples M_{0x_i} or M_{0y_i}, applied on the stiffeners as shown in Fig. 4. The four-point

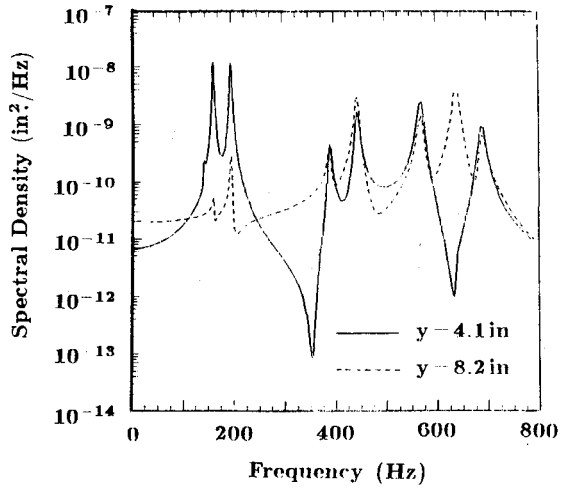

Fig. 5 Deflection response spectral densities to point forces for a composite panel.

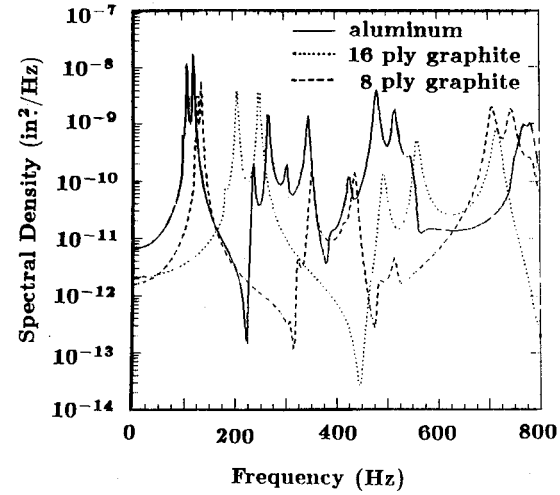

Fig. 6 Deflection response spectral densities for different material characteristics.

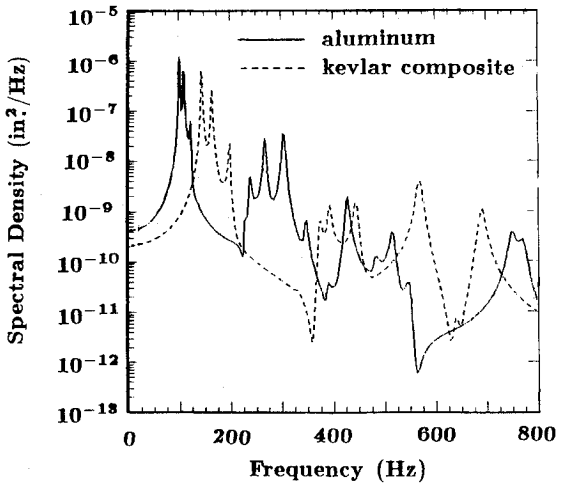

Fig. 7 Deflection response spectral densities to point couples M_{0y}.

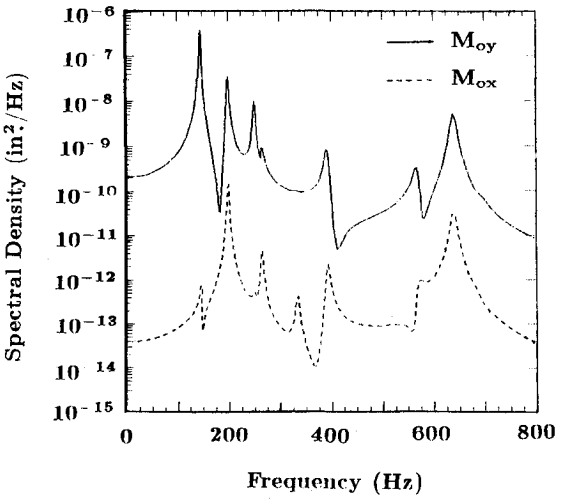

Fig. 8 Deflection response spectral densities to different point couple inputs for a composite panel.

forces or point couples are assumed to be characterized by truncated Gaussian white noise spectral densities

$$S_{F_i}(f) = \begin{cases} 0.00084 \text{ lb}^2/\text{Hz} & 0 \le f \le f_u \\ 0 & \text{otherwise} \end{cases} \quad (33)$$

$$S_{M_{0i}}(f) = \begin{cases} 0.00084 \text{ (lb} - \text{in.)}^2/\text{Hz} & 0 \le f \le f_u \\ 0 & \text{otherwise} \end{cases} \quad (34)$$

where f is the frequency in Hz, $i = 1,2,3,4$ and f_u is the upper cut-off frequency. These point loads are located at the positions as indicated in Fig. 4.

Response of a Stiffened Composite Panel

Deflection response spectral densities of the composite panel were obtained to point forces. The results are for an upper cutoff frequency $f_u = 800$ Hz. The stiffened panel has free boundary conditions at $y = 0, L_y$ (the ends are supported by the end stiffeners) as shown in Fig. 4. The panel deflection response shown in Fig. 5 is calculated at $x = 10$ in., $y = 4.1$ in. and $y = 8.2$ in. The first point is at the middle of the first panel

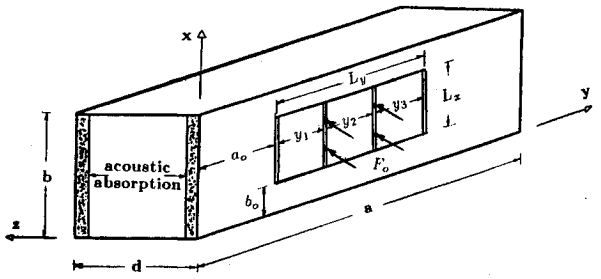

Fig. 9 Geometry of an acoustic enclosure subject to random point loads.

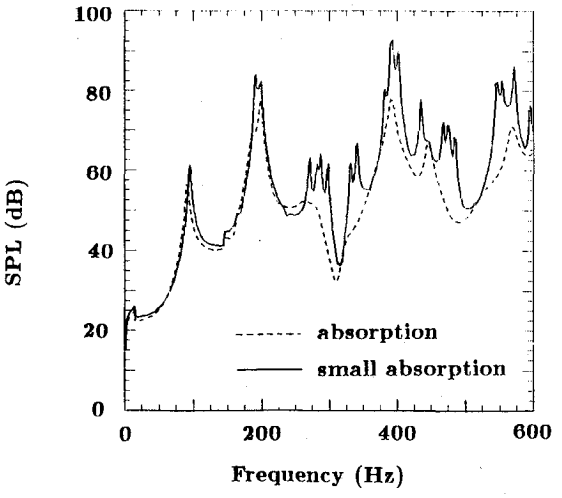

Fig. 10 Sound pressure levels in the interior for different acoustic absorption characteristics.

bay, and the second point is at the middle of the first stringer. The composite panel consists of 16 plies of kevlar with the stacking sequence, $[0/90/45/-45]_{2s}$. Depending on the value of frequency, significant differences in response values are obtained at different locations of the composite panel. In Fig. 6 a comparison between an aluminum panel and a composite (graphite) panel is presented. The response was calculated at $x = 10$ in., $y = 4.1$ in. The stacking sequence for the 8- and 16-ply composite is $[0/90/45/-45]_{s,2s}$. A significant amount of response reduction can be achieved by using composite materials. The 8-ply composite has the same thickness as the aluminum panel but almost one half of its weight. It is noted that the fundamental frequency of the vibration for the 8-ply graphite is lower than the 16-ply graphite panel as expected.

Spectral densities were also obtained to point couples as shown in Fig. 4. In Fig. 7 a direct comparison between aluminum and kevlar composite (16 plies) is presented. The response is calculated at $x = 10$ in., $y = 4.1$ in., and ply stacking sequence is the same as in Fig. 6, and the point couples M_{0y} are acting in a $-y$ direction. From the results presented in Figs. 6 and 7, differences can be seen in the skin-stringer panel response between point force and point couple inputs. The effect of direction of the input point couple action is illustrated in Fig. 8. The dashed line gives skin-stringer panel response at point $x = 5$ in., $y = 12.3$ in. for M_{0x} input (bending effect on the stringers), and the solid line is for M_{0y} (twisting effect on the stringers) input. The material is kevlar with 16 plies, and the stacking sequence is the same as in Fig. 6. These results indicate that the deflection response is significantly smaller for bending moment input M_{0x} than for twisting moment input M_{0y}. This is due to the fact that these stiffeners provide more resistance in bending than in torsion. In addition, it is evident that by choosing stiffeners with a different cross section that

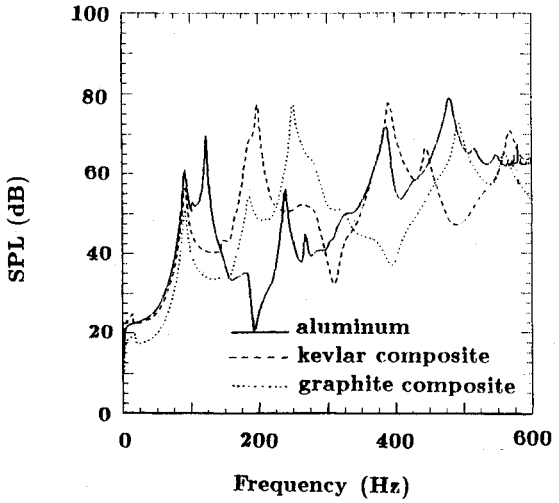

Fig. 11 Sound pressure levels for different material characteristics of the flexible surface.

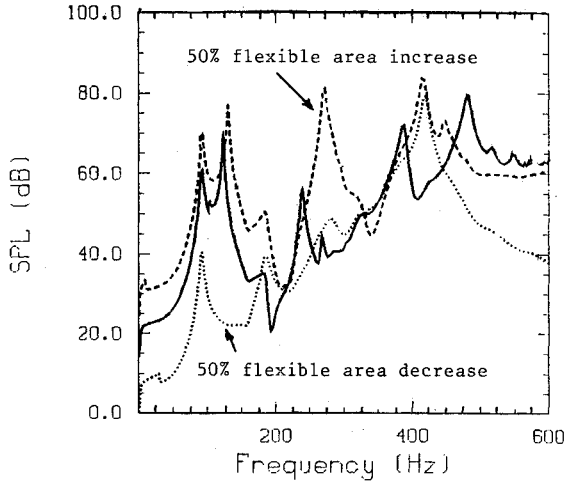

Fig. 13 Sound pressure levels in the interior for different size of the flexible surface.

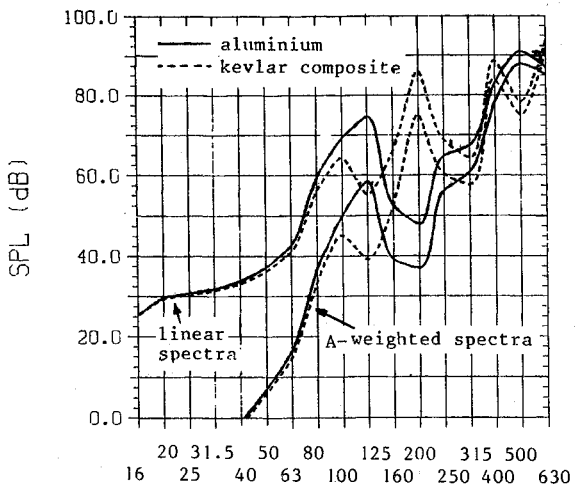

Fig. 12 One-third octave sound pressure levels in the interior.

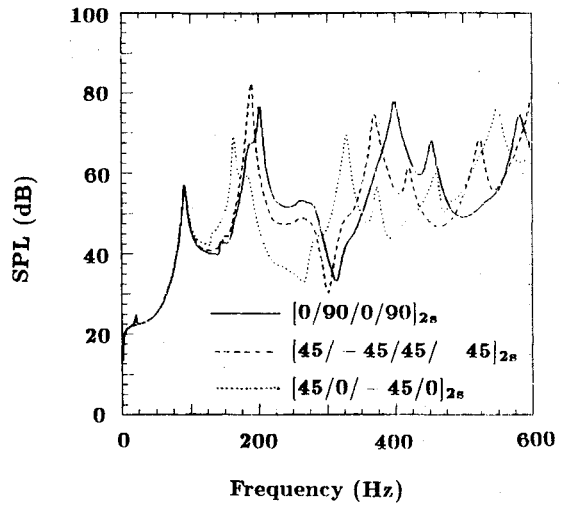

Fig. 14 Sound pressure levels for different fiber orientation of a composite stiffened panel.

offers more resistance in torsion, the response can be reduced. In general, by tailoring the geometric characteristics, desired response levels can be obtained.

Sound Transmission

For the calculation of noise transmission into the enclosure, a simplified model shown in Fig. 9 has been chosen. The stiffened panel is again composed of three equal bays. The elastic structure is attached to the enclosure with a simple support at $x = b_0$, $x = b_0 + L_x$ and $y = a_0$, $y = a_0 + L_y$. Random point loads are acting at the stiffeners. The walls at $z = 0$ and $z = d$ of the acoustic enclosure are treated with absorbtive materials, which are represented by the point impedance model as

$$Z_A(\omega) = Z_R + iZ_I \tag{35}$$

where for acoustic materials, the resistance Z_R and the reactance Z_I are given by[21]

$$Z_R = \rho c_0 \left[1 + 0.0571 \left(\frac{2\pi R}{\rho \omega} \right)^{0.754} \right] \tag{36}$$

$$Z_I = -\rho c_0 \left[0.087 \left(\frac{2\pi R}{\rho \omega} \right)^{0.732} \right] \tag{37}$$

in which ρc_0 is the characteristic impedance, and R is the flow resistivity of the absorbing materials. The results presented in this paper are obtained for resistivity $R = 4 \times 10^4$ mks rayls/m and for bulk reaction coefficient $B(\omega) = 0$.

The numerical results were obtained for $a = 142$ in., $b = 50$ in., $d = 48$ in., $a_0 = 60$ in., $b_0 = 15$ in., $y_1 = y_2 = y_3 = 8.2$ in., $L_x = 20$ in., $L_y = 24.6$ in. Interior noise in the enclosure was calculated at $x = 25$ in., $y = 71$ in., and $z = 24$ in. The acoustic damping coefficient β was related to the acoustic modal damping ratios ξ_{ij} by

$$\xi_{ij} = \frac{\beta c_0^2}{2\omega_{ij0}} \tag{38}$$

where $\beta c_0^2 = 2\omega_0 \xi_0$, in which ω_0 is the lowest acoustic modal frequency chosen from ω_{001}, ω_{010} and ω_{100} (i.e., ω_{010} in this case). The damping ratio corresponding to the fundamental acoustic mode, $\xi_0 = 0.03$, takes into account the contributions of all the damping effects of the acoustic space. Air density

and speed of sound in the enclosure are $\rho = 1.147 \times 10^{-7}$ $lb_f.s^2/in.^4$ and $c_0 = 13540$ in./s, respectively. All the calculations are based on a frequency bandwidth $\Delta f = 1$ Hz.

Sound pressure levels are given in Fig. 10 for an acoustic enclosure with a small amount of absorption at the walls ($Z_A \to \infty$) and for the case where the walls are treated with porous materials for which the point impedance is given in Eqs. (35–37). The stiffened laminated composite panel (flexible surface) has 16 plies with stacking sequence $[0/90/45/-45]_{2s}$, and the material is kevlar. The inputs to the stiffened panel are four point forces acting on the two intermediate stringers (Fig. 9) for which the spectral densities are given in Eq. (33). As can be observed from these results, the peaks of the acoustic modes are suppressed when the acoustic absorption in the interior is large.

A comparison of the sound pressure levels for different materials of the flexible surface is given in Fig. 11. The comparison is between aluminum and composite panels with 16 plies made of kevlar and graphite. As can be observed from these results, the transmitted noise is a function of the type of vibrating flexible surface. A comparison between aluminum and kevlar composite panels is presented in Fig. 12. The results are plotted on a 1/3-octave scale (linear and A-weighted). The noise levels generated by a composite panel are higher than the noise levels for an aluminum panel at higher frequencies. For a stiffened panel, a shift in modal frequency could induce different coupling between structural and acoustic modes.

The results shown in Fig. 13 indicate the effect of the flexible surface size. The panels are 16-ply kevlar composite with the same stacking sequence as before. The sizes of the flexible surface are $L_x = 20.0$ in., $y_i = 8.2$ in. (solid); $L_x = 24.5$ in., $y_i = 10.0$ in. (dashed), which corresponds to a 50% area increase; $L_x = 14.2$ in., $y_i = 5.8$ in. (dotted), which corresponds to a 50% area decrease. It is seen that the transmitted sound levels are higher as the area of the stiffened panel increases.

The results presented in Fig. 14 correspond to a 16-ply composite made of kevlar with different stacking sequences. The loading conditions and all the other characteristics are the same for all the cases. The fiber orientation is described in Fig. 12. These results show that interior noise is a function of fiber orientation in a composite stiffened panel. The interior noise levels may be tailored to meet specific needs by selecting a suitable fiber orientation.

Conclusions

Transfer matrix procedures were developed to study the dynamic response, noise generation, and transmission of stiffened composite panel. The formulation can be applied to a variety of discretely stiffened composite and isotropic structures. In addition, it has been shown that structural response and transmitted noise levels in the interior are sensitive to the dynamic characteristics of the stiffened sidewall. It was found that the stiffened panel response is strongly dependent on the location and the forcing function and the rigidity of the stiffeners. In general, the response levels for a composite stiffened panel are lower than those of an equivalent aluminum stiffened panel. The interior noise is strongly dependent on the absorption of the interior walls, the area of the vibrating surface, and the fiber orientation of the flexible surface. A fiber reinforced composite flexible surface tends to generate more noise at higher frequencies than the aluminum panel. However, the differences are small when overall levels are compared. The results indicate that by tailoring the geometric and material characteristics of structural components, the vibration levels and noise transmission can be reduced.

Appendix: Field Transfer Matrices

The field transfer matrices for the composite panel can be expressed as

$$[F]_j = [B]_j[R]_j[B]_j^{-1} \tag{A1}$$

where

$$[B] = \begin{bmatrix} 1 & 0 & 0 & 0 \\ 0 & 1 & 0 & 0 \\ -D_{12}\left(\frac{n\pi}{L_x}\right) & 0 & D_{22} & 0 \\ 0 & -(D_{12}+4D_{66})\left(\frac{n\pi}{L_x}\right)^2 & 0 & D_{22} \end{bmatrix} \tag{A2}$$

and

$$[B]^{-1} = \begin{bmatrix} 1 & 0 & 0 & 0 \\ 0 & 1 & 0 & 0 \\ \frac{D_{12}}{D_{22}}\left(\frac{n\pi}{L_x}\right)^2 & 0 & \frac{1}{D_{22}} & 0 \\ 0 & \frac{D_{12}+4D_{66}}{D_{22}}\left(\frac{n\pi}{L_x}\right)^2 & 0 & \frac{1}{D_{22}} \end{bmatrix} \tag{A3}$$

Following the procedures of Refs. 12 and 14, matrix $[R]$ is

$$[R] = \begin{bmatrix} C_0 & S_{-1} & C_{-2} & S_{-3} \\ S_1 & C_0 & \tilde{S}_{-1} & C_{-2} \\ C_2 & S_1 & \tilde{C}_0 & \tilde{S}_{-1} \\ S_3 & C_2 & \tilde{S}_1 & \tilde{S}_0 \end{bmatrix} \tag{A4}$$

in which

$$f_{0n}(y) = C_0 = s_n^2(\sigma_{2n}^2 \cosh\sigma_{1n}y + \sigma_{1n}^2 \cos\sigma_{2n}y) \tag{A5}$$

$$f_{1n}(y) = S_{-1} = s_n^2\left(\frac{\sigma_{2n}^2}{\sigma_{1n}} \sinh\sigma_{1n}y + \frac{\sigma_{1n}^2}{\sigma_{2n}} \sin\sigma_{2n}y\right) \tag{A6}$$

$$f_{2n}(y) = C_{-2} = s_n^2(\cosh\sigma_{1n}y - \cos\sigma_{2n}y) \tag{A7}$$

$$f_{3n}(y) = S_{-3} = s_n^2\left(\frac{1}{\sigma_{1n}} \sinh\sigma_{1n}y - \frac{1}{\sigma_{2n}} \sin\sigma_{2n}y\right) \tag{A8}$$

$$\tilde{C}_0 = s_n^2(\sigma_{1n}^2 \cosh\sigma_{1n}y + \sigma_{2n}^2 \cos\sigma_{2n}y) \tag{A9}$$

$$C_2 = s_n^2\sigma_{1n}^2\sigma_{2n}^2(\cosh\sigma_{1n}y - \cos\sigma_{2n}y) \tag{A10}$$

$$\tilde{S}_{-1} = s_n^2(\sigma_{1n} \sinh\sigma_{1n}y + \sigma_{2n} \sin\sigma_{2n}y) \tag{A11}$$

$$S_1 = s_n^2\sigma_{1n}\sigma_{2n}(\sigma_{2n} \sinh\sigma_{1n}y - \sigma_{1n} \sin\sigma_{2n}y) \tag{A12}$$

$$\tilde{S}_1 = s_n^2(\sigma_{1n}^3 \sinh\sigma_{1n} - \sigma_{2n}^3 \sin\sigma_{2n}y) \tag{A13}$$

$$S_3 = s_n^2\sigma_{1n}^2\sigma_{2n}^2(\sigma_{1n} \sinh\sigma_{1n}y + \sigma_{2n} \sin\sigma_{2n}y) \tag{A14}$$

$$s_n^2 = \frac{1}{\sigma_{1n}^2 + \sigma_{2n}^2} \tag{A15}$$

Acknowledgment

Dr. C. Lyrintzis was supported in part by a grant from the San Diego State University Foundation.

References

[1]NASA, "*Space Station Program. Description, Applications and Opportunity*," Noyes Publicatiaons, 1983.

[2]Wensley, D. C., "Space Station Architecture and Configuration," *AIAA Annual Meeting,* Washington D.C., May 1–3, 1984.

[3]Davis, G. W., and Sakada, I. F., "Design Considerations for Composite Fuselage Structure of Commercial Transport Aircraft," NASA CR-159296, March 1981.

[4]"Composites," *Aviation Week and Space Technology,* Oct. 12, 1987, pp. 49–54.

[5]Mixson, J. S., and Wilby, J. F., "Airplane Interior Noise: A Status Review," AIAA Paper 87-2659, October 1987.

[6]Vaicaitis, R., and Mixson, J. S., "Review of Research on Structureborne Noise," *Proceedings of the AIAA/ASME/ASCE/AHS 26th Structures, Structural Dynamics and Materials Conference,* Paper 85-0786-CP, AIAA, New York, April 1985.

[7]Sen Gupta, G., Landmann, A. E., Mera, A., and Yantis, T. F., "Prediction of Structure-Borne Noise Based on the Finite Element Method," AIAA Paper 86-1861, July 1986.

[8]Roussos, L. A., Powell, C. A., Grosveld, F. W., and Koval, L. R., "Noise Transmission Characteristics of Advanced Composite Structural Materials," *Journal of Aircraft,* Vol. 21, No. 7, 1984, pp. 528–535.

[9]Bofilios, D. A., and Vaicaitis, R., "Response of Double Wall Composite Shells to Random Point Loads," *Journal of Aircraft,* Vol. 24, No. 4, 1987, pp. 268–273.

[10]Vaicaitis, R., and Bofilios, D. A., "Noise Transmission of Double Wall Composite Shells," AIAA Paper 86-1937, July 1986.

[11]Lyrintzis, C. S., and Vaicaitis, R., "Structure-Borne Noise Generation and Transmission," *Journal of Probalistic Engineering Mechanics,* Vol. 2, No. 3, Sept. 1987, pp. 114–120.

[12]Lyrintzis, C. S., "Response of Discretely Stiffened Structures and Transmission of Structure-Borne Noise," Ph.D Dissertation, Dept. of Civil Engineering and Engineering Mechanics, Columbia Univ., New York, N.Y., 1987.

[13]Vaicaitis, R., and Lyrintzis, C. S., "Response of Discretely Stiffened Structures," AIAA Paper 87-0914, April 1987.

[14]Lin, Y. K., and Donaldson, B. K., "A Brief Survey of Transfer Matrix Techniques with Special Reference to Aircraft Panels," *Journal of Sound and Vibration,* Vol. 10, No. 1, 1969, pp. 103–143.

[15]Vaicaitis, R., and Choi, S. T., "Response of Stiffened Panels for Applications to Acoustic Fatique," AIAA Paper 87-2711, Oct. 19–21, 1987.

[16]Comte-Bellot, G., and Gay, B., "Vibration Analysis of Skin-Stringer Structures by the Super Matrix Method," AIAA Paper 87-2734, Oct. 1987.

[17]Jones, R. M., *Mechanics of Composite Materials,* Scripta, Washington D.C., 1975.

[18]Vinson, J. R., and Sierakowski, R. L., *The Behavior of Structures Composed of Composite Materials,* Kluwer Publishers, Hingham, MA, 1986.

[19]Timoshenko, S. and Woinowsky-Krieger, S., *Theory of Plates and Shells,* McGraw-Hill, New York, 1959.

[20]Vaicaitis, R. and Slazak, M., "Noise Transmission Through Stiffened Panels," *Journal of Sound and Vibration,* Vol. 70, No. 3, 1980, pp. 413–426.

[21]Beranek, L. L., ed., *Noise and Vibration Control,* McGraw-Hill, New York, 1971.

[22]Bliss, D. B., "Study of Bulk Reacting Porous Sound Absorbers and a New Boundary Condition for Thin Porous Layers," *Journal of the Acoustical Society of America,* Vol. 71, No. 3, March 1982, pp. 533–545.

[23]Dowell, E. H., and Voss, H. M., "The Effect of Cavity on Panel Vibrations," *American Institute of Aeronautics and Astronautics Journal,* Vol. 1, 1963, pp. 476–478.

[24]Nafske, D. J., and Sung, S. H., "Structural-Acoustic System Analysis Using the Modal Synthesis Technique," *Proceedings of the 3rd International Modal Analysis Conference,* Orlando, Florida, Jan. 1985.